nature neuroscience

Stimulus-specific enhancement of fear extinction during slow-wave sleep

Katherina K Hauner, James D Howard, Christina Zelano & Jay A Gottfried

Sleep can strengthen memory for emotional information, but whether emotional memories can be specifically targeted and modified during sleep is unknown. In human subjects who underwent olfactory contextual fear conditioning, re-exposure to the odorant context in slow-wave sleep promoted stimulus-specific fear extinction, with parallel reductions of hippocampal activity and reorganization of amygdala ensemble patterns. Thus, fear extinction may be selectively enhanced during sleep, even without re-exposure to the feared stimulus itself.

Sleep represents a critical period for memory consolidation in which new memories are highly labile and vulnerable to modulation[1,2]. Episodic and procedural memories learned while awake and in the presence of a context (for example, smell or sound) can be reactivated and enhanced via re-presentation of the same context during slow-wave sleep (SWS)[2–5]. Sleep is also important for the consolidation of emotional memory[6,7], although the underlying neural mechanisms are poorly understood. In particular, it is unknown whether emotional memories can be actively modulated during sleep and, if so, which brain areas would support these changes. Furthermore, whether specific emotional memories can be individually targeted during sleep has been similarly unexplored, despite the potential implications of such research for treatment of pathological fear and for understanding the neuroplasticity of emotional memory storage.

We combined high-resolution functional magnetic resonance imaging (fMRI) with physiological recordings to test whether conditioned fear memories are selectively modulated during SWS. Healthy human subjects ($n = 15$) underwent olfactory contextual conditioning in which face images (conditioned stimuli, CS+) were paired with mild electric shocks (unconditioned stimuli, US) in the presence of background odorants, one of which was re-presented during SWS to reactivate the associated CS+ representation in the absence of reinforcement (US; **Supplementary Fig. 1**). Odorant stimuli were selected as contexts because of their reliability as sensory cues that can be administered unobtrusively during sleep[4,8]. Given that contextual extinction reduces fear responses to an associated CS+[9], our central hypothesis was that unreinforced exposure to a fear-conditioned context during sleep would promote fear extinction, indexed via changes in physiological arousal. On the basis of prior work on olfactory-related fear extinction[10] and related studies[2,11], we considered that sleep-based reactivation might elicit targeted changes in hippocampus, amygdala and prefrontal cortex, as well as piriform cortex, insula and anterior cingulate.

During contextual fear conditioning (**Supplementary Fig. 1**), subjects were conditioned to two face images (CS+): a target CS+ (tgCS+), presented only in the context of a target odorant (indicating later delivery during sleep), and a non-target CS+ (ntCS+), presented only in the context of a distinct non-target odorant (not delivered during sleep). Under a partial reinforcement schedule, 50% of all CS+ were paired with shock (US) and 50% were unpaired, with only unpaired CS+ included in analyses (Online Methods). Two additional face images (one in each context) were never paired with the US (tgCS−, ntCS−) and served as context-specific control stimuli. Successful fear conditioning was evidenced by increased stimulus-evoked skin-conductance response (SCR) for tgCS+ and ntCS+ in comparison to the respective CS− baselines ($t_{14} = 2.56$, $P = 0.02$, two-tailed unless otherwise noted), with no effects of odorant context (context (target, non-target) × CS (+, −), $F_{1,14} = 1.17$, $P = 0.30$). In parallel, increased activation to CS+ (versus CS−) was observed in regions that have been implicated in olfactory and contextual conditioning[10,11], including orbitofrontal cortex (OFC), insula, anterior cingulate cortex (ACC) and hippocampus (all $P \leq 0.001$; **Supplementary Table 1**), and at lower threshold in right amygdala ($P = 0.009$).

Following fear conditioning, subjects exited the MRI scanner to begin the nap phase of the experiment (duration = 73 ± 4 min, mean ± s.e.m.). When subjects entered SWS (17 ± 3 min), the target odorant was continuously delivered in the absence of the US, providing non-reinforced re-exposure to the conditioned context. During the first half of SWS, presentation of odorant (versus alternating odorant-off intervals) elicited a robust SCR (**Fig. 1a**); however, as odorant delivery continued into the second half of SWS, SCR declined ($t_{13} = -2.43$, $P = 0.03$, one tailed). These findings are consistent with the notion that re-exposure to the target context during sleep induced within-session fear extinction. Notably, comparison of odorant-evoked SCR to alternating odorant-off epochs ensured specificity of these effects to odorant presentation, minimizing potential confounds of generalized habituation or SCR signal fatigue. Subjects did not awaken during odorant delivery, as confirmed by polysomnography and spectral analysis (**Supplementary Fig. 2**), nor were they later able to identify the target odorant above chance (Online Methods).

On awakening, subjects returned to the MRI scanner and underwent a post-sleep task that mirrored pre-sleep conditioning. Odorant re-exposure during SWS weakened expression of conditioned fear in the post-sleep period. This effect was stimulus specific: SCR reduction from pre- to post-sleep was preferentially greater in response to tgCS+ versus ntCS+, both as a main effect ($t_{14} = -2.11$, $P = 0.05$, one-tailed) and when adjusted for the respective effects of tgCS− and ntCS− ($t_{14} = -2.31$, $P = 0.04$, one-tailed) (**Fig. 1b**). Notably, the

Department of Neurology, Feinberg School of Medicine, Northwestern University, Chicago, Illinois, USA. Correspondence should be addressed to K.K.H. (hauner@u.northwestern.edu).

Received 12 June; accepted 29 August; published online 22 September 2013; doi:10.1038/nn.3527

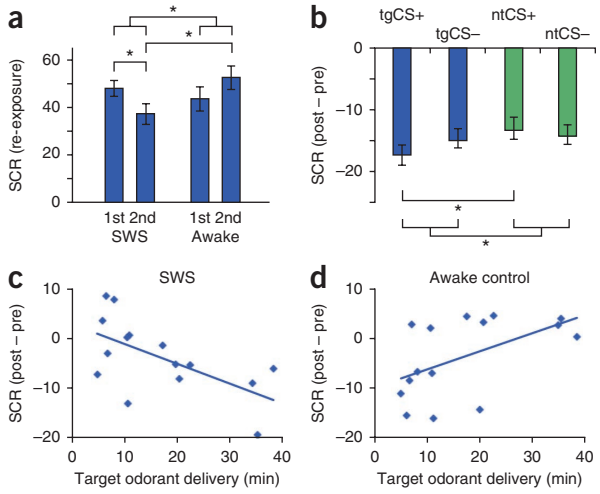

Figure 1 Behavioral results. (**a**) During target odorant re-exposure, SCR decreased from the first half of re-exposure to the second half (compared with odorant-off control periods) for subjects in SWS (left). In comparison, SCR increased during this period for awake control subjects (right). $^*P \leq 0.05$, one-tailed. Bar plots represent mean SCR activity (percentage-change units). Error bars represent s.e.m. (adjusted for between-subjects differences; Online Methods). (**b**) From pre-sleep to post-sleep, mean SCR was selectively reduced for the target (sleep-reactivated) CS+ (tgCS+ versus ntCS+). Negative values denote pre- to post-sleep reductions. $^*P \leq 0.05$, one-tailed. Error bars represent s.e.m. (**c**) Duration of contextual re-exposure in SWS predicted SCR reductions from pre- to post-sleep ($r = -0.61$, $P = 0.02$, tgCS+ versus ntCS+, adjusted for CS– baselines). Each dot represents one subject. (**d**) In awake subjects, re-exposure duration predicted subsequent increases in SCR ($r = 0.53$, $P = 0.04$). Re-exposure duration was yoked between experimental sleep (**c**) and awake (**d**) groups.

magnitude of SCR reduction correlated with the duration of odorant re-exposure across subjects ($r = -0.61$, $P = 0.02$, $n = 15$; **Fig. 1c**), whereby prolonged re-exposure resulted in stronger fear extinction to tgCS+ (versus ntCS+). The specificity of these results for the target (versus non-target) condition excludes the possibility of nonselective effects of SWS or odorant re-exposure *per se*.

To establish whether this effect was specific to the sleep condition, we repeated the same procedure in a follow-up behavioral experiment, using an independent group of awake subjects ($n = 15$) who viewed a documentary film during odorant re-exposure (in place of a nap). Duration of odorant re-exposure was yoked between awake and sleep subjects, ensuring that this variable was identical across groups. A between-groups comparison of SCR during odorant re-exposure revealed that the SCR reduction (from first to second half of re-exposure) was specific to the sleep condition (group × half, $F_{1,24} = 4.23$, $P = 0.05$), with significant main effects in the second half of re-exposure (sleep < awake, $t_{11} = -2.58$, $P = 0.03$, one-tailed) (**Fig. 1a**). Specificity of contextual re-exposure effects for the sleep condition was further confirmed by the interaction of group (sleep, awake) and stimulus (tgCS+, ntCS+) when re-exposure duration was entered as a covariate ($F_{2,24} = 8.82$, $P = 0.006$). Direct comparison between sleep (**Fig. 1c**) and awake groups (**Fig. 1d**) established that the correlation between re-exposure duration and condition-specific fear extinction was also specific to the sleep group ($z = 3.18$, $P = 0.002$, Fisher r-to-z transformation). These results suggest that sleep may constitute a unique state in which targeted fear memories can be selectively extinguished while non-targeted memories are left intact.

Next, we used fMRI to examine how sleep-mediated fear extinction is implemented in the human brain. A key region of interest was the hippocampal formation, which is involved in contextual fear conditioning[11,12] and retrieval[13] and in SWS-mediated memory consolidation[2,5]. Whole-brain analyses revealed a decline in stimulus-evoked mean fMRI activity for tgCS+ (versus ntCS+) from pre- to post-sleep in right anterior hippocampus ($P = 0.0003$, cross-validated, small-volume corrected; **Fig. 2a**), ACC and insula (**Supplementary Table 2**). Furthermore, odorant re-exposure duration (during SWS) was negatively correlated with tgCS+-evoked activity in right entorhinal cortex ($r = -0.51$, $P = 0.05$, cross-validated; **Fig. 2b**), a region that provides substantial afferent input to hippocampus[14]. These reductions in fMRI activity are consistent with the roles of these regions in contextual retrieval (hippocampus, entorhinal cortex)[13] and expression (ACC, insula)[10] of fear memory.

In a final analysis, we used multivariate fMRI pattern techniques to test whether re-exposure to the fear context during sleep would induce a fundamental shift in CS+ meaning, namely, from a representation of conditioned fear to a representation of extinguished fear (**Fig. 2c**). In such a case, one would expect cue-evoked patterns of fMRI ensemble activity in pre-sleep and post-sleep to diverge specifically for the target (sleep reactivated) CS+. As hypothesized, multivariate analysis revealed that pre- and post-sleep patterns evoked by tgCS+ were decorrelated in left amygdala (context (target, non-target) × CS (+, −), $F_{1,14} = 7.06$, $P = 0.02$). A similar trend was observed when left and right amygdala were considered together ($F_{1,14} = 4.31$, $P = 0.057$), whereas a lack of pattern-based changes in piriform cortex, OFC and fusiform cortex (all $P > 0.29$) underscored the regional specificity of this effect.

Our findings provide robust evidence that re-exposure to an unreinforced fear context during sleep enhances fear extinction in a stimulus-selective manner. Mechanistically, it is difficult to conclude whether enhancement of fear extinction was a result of fear 'unlearning' (erasure), in which associative strength between the CS+ and US is weakened[15], or 'new learning' of an association between the CS+ and absence of the US[16]. The latter interpretation appears to be more consistent with our multivariate analyses (**Fig. 2c**), which suggest that contextual re-exposure in SWS induced the formation of a qualitatively unique memory trace in the amygdala[17] rather than simply weakening or eliminating the original trace.

Notably, pattern-based amygdala changes were accompanied by reduced hippocampal activity at post-sleep retrieval, an effect that was selective for the stimulus targeted during re-exposure (tgCS+; **Fig. 2a**). One interpretation of this finding can be drawn from reports that sleep-based reactivation of non-emotional memories results in accelerated memory consolidation (in other words, improved retrieval)[3,4], which has been associated with decreased hippocampal dependence[18]. Although our study had no direct test of explicit memory for the conditioned stimuli, analysis of response times to conditioned stimulus presentations (as an indirect assessment of stimulus recognition, Online Methods) indicated that increased re-exposure to the target context during SWS led to faster recognition of the tgCS+ image ($r = -0.63$, $P = 0.02$; tgCS+ versus ntCS+, adjusted for CS– baselines). We therefore propose that re-exposure to the target odorant context during SWS, in absence of the US (shock), accelerated memory consolidation for the unreinforced tgCS+, resulting in less hippocampal dependence for encoding the tgCS+ (**Fig. 2a**), improved memory performance for the tgCS+, as indexed via reduced reaction times, and weakened expression of fear (enhanced SCR extinction) to the tgCS+ (**Fig. 1b**,**c**).

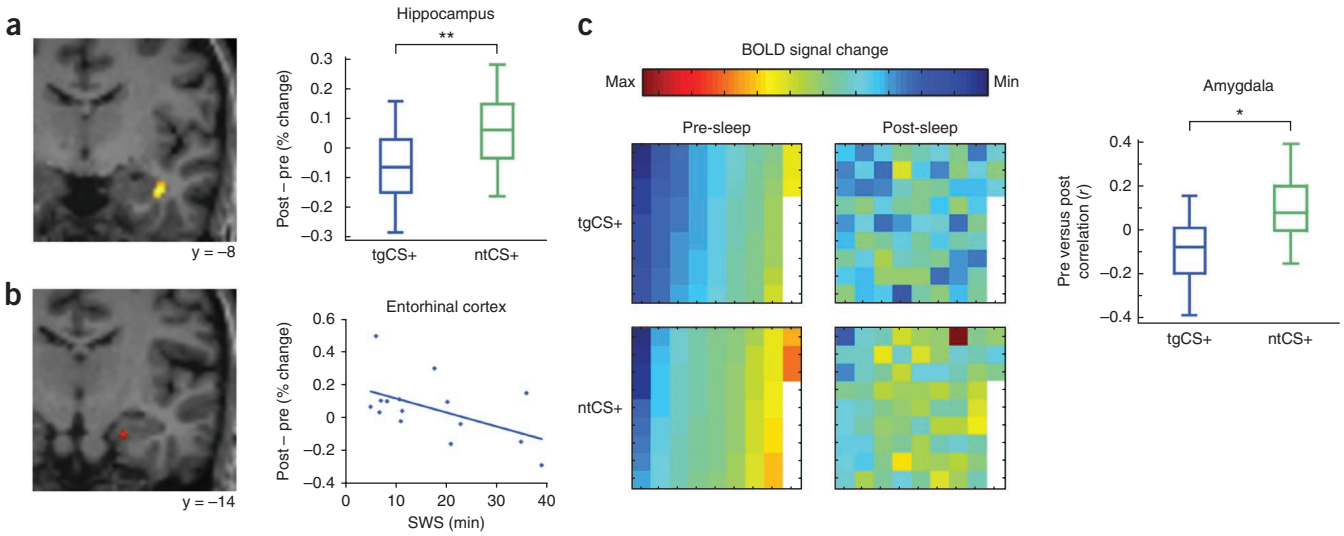

Figure 2 Sleep-related modulatory effects of target odorant re-exposure on fMRI activity. (**a**) Activity evoked by tgCS+ (versus ntCS+) was reduced from pre- to post-sleep in anterior hippocampus ($t_{14} = -4.65$, $^{**}P < 0.001$; adjusted for CS– baselines). Activation maps are overlaid on a T1-weighted coronal section from a representative subject (display threshold, $P < 0.005$). Box plots (right) indicate median (central line) and upper and lower quartiles (top and bottom of box) for each condition. Whiskers denote the extent of data between the 10th and 90th percentiles. (**b**) Post-sleep (versus pre-sleep) activity in entorhinal cortex evoked by tgCS+ (versus ntCS+) was negatively correlated with the duration of odorant re-exposure during SWS ($r = -0.51$, $P = 0.05$, $n = 15$). (**c**) Voxel-wise ensemble maps (left) of activity in left amygdala from one subject revealed that condition-specific patterns diverged more for tgCS+ (versus ntCS+) from pre- to post-sleep. Each square represents signal intensity from a different voxel ($n = 75$), arranged in columns from top left to bottom right in ascending order for tgCS+ in the pre-sleep condition. Across all subjects (right), pre- and post-sleep pattern ensembles in amygdala became more distinct (less correlated) for tgCS+ compared to ntCS+ ($t_{14} = -2.66$, $^{*}P = 0.02$,; adjusted for CS– baselines, paired t test).

That fear extinction was not observed in the awake group is somewhat paradoxical. One possibility is that fear responses may be enhanced when the delay between conditioning and extinction is brief[19]. Thus, the use of a short delay in our study (as in other sleep reactivation procedures[3]) may have selectively promoted fear expression for the awake group. As a form of 'pseudo-conditioning', this effect could arise if the contextual odorant had reactivated the US memory or, alternatively, the association between the tgCS+ and US. Another possible explanation for the discrepant results between sleep and awake groups is that the hippocampus may be relatively disengaged from encoding during sleep (compared with wakefulness)[20]. Thus, odorant re-exposure would have greater effects on consolidation of fear extinction in SWS, when hippocampal encoding is effectively offline. In this manner, divergent effects of sleep versus wakefulness may relate to hippocampal disengagement (during SWS) that impedes encoding of recently learned information, rather than to effects of sleep *per se*.

Taken together, our results demonstrate that SWS may represent a unique period during which fear memory consolidation can be preferentially influenced by exogenously delivered cues. Our findings suggest that the process of enhancing fear extinction can be accomplished without conscious perception of the re-exposed context, or even without conscious awareness of any task component. The capacity to target, and thereby reactivate, specific emotional memories during sleep provides new insights into the plasticity of emotional memory storage and underscores the potential for future translational research in this area.

METHODS

Methods and any associated references are available in the online version of the paper.

Note: Any Supplementary Information and Source Data files are available in the online version of the paper.

ACKNOWLEDGMENTS

We thank P. Zee, C. Westerberg and K.N. Wu for technical assistance, and J. Radulovic and K. Paller for insightful discussions. Support was provided from the US National Institutes of Health to K.K.H. (F32MH091967, T32NS047987) and to J.A.G. (R01DC010014, R21DC012014), and from the Northwestern University Center for Translational Imaging.

AUTHOR CONTRIBUTIONS

K.K.H. conceived the experiment. K.K.H. and J.A.G. designed the research. K.K.H. conducted the research and analyzed the data. J.D.H. performed multivariate analyses. C.Z. performed spectral power analysis. All of the authors prepared the manuscript.

COMPETING FINANCIAL INTERESTS

The authors declare no competing financial interests.

1. Walker, M.P. & Stickgold, R. *Neuron* **44**, 121–133 (2004).
2. Diekelmann, S., Buchel, C., Born, J. & Rasch, B. *Nat. Neurosci.* **14**, 381–386 (2011).
3. Antony, J.W. *et al. Nat. Neurosci.* **15**, 1114–1116 (2012).
4. Rasch, B., Buchel, C., Gais, S. & Born, J. *Science* **315**, 1426–1429 (2007).
5. Bendor, D. & Wilson, M.A. *Nat. Neurosci.* **15**, 1439–1444 (2012).
6. Barnes, D.C., Chapuis, J., Chaudhury, D. & Wilson, D.A. *PLoS ONE* **6**, e18130 (2011).
7. Payne, J.D. & Kensinger, E.A. *J. Cogn. Neurosci.* **23**, 1285–1297 (2011).
8. Arzi, A. *et al. Nat. Neurosci.* **15**, 1460–1465 (2012).
9. Stout, S.C. & Miller, R. *Behav. Processes* **66**, 7–16 (2004).
10. Gottfried, J.A. & Dolan, R.J. *Nat. Neurosci.* **7**, 1144–1152 (2004).
11. Anagnostaras, S.G., Gale, G.D. & Fanselow, M.S. *Hippocampus* **11**, 8–17 (2001).
12. Milad, M.R. *et al. Biol. Psychiatry* **62**, 446–454 (2007).
13. Hobin, J.A., Ji, J. & Maren, S. *Hippocampus* **16**, 174–182 (2006).
14. Burwell, R.D. & Amaral, D.G. *J. Comp. Neurol.* **398**, 179–205 (1998).
15. Han, J.H. *et al. Science* **323**, 1492–1496 (2009).
16. Bouton, M.E. *Biol. Psychiatry* **52**, 976–986 (2002).
17. Herry, C. *et al. Nature* **454**, 600–606 (2008).
18. Wang, S.H., Teixeira, C.M., Wheeler, A.L. & Frankland, P.W. *Nat. Neurosci.* **12**, 253–255 (2009).
19. Huff, N.C., Hernandez, J.A., Blanding, N.Q. & LaBar, K.S. *Behav. Neurosci.* **123**, 834–843 (2009).
20. Mednick, S.C. *et al. Trends Neurosci.* **34**, 504–514 (2011).

ONLINE METHODS

Sleep group. 18 subjects provided written informed consent to participate in the study, which was approved by the Institutional Review Board of Northwestern University. Exclusionary criteria included a history of significant medical or psychiatric illness, history of sleep disorder, current psychotropic medication use, recent (<4 weeks) nasal infection, evidence of 'mouth breathing' while awake or asleep, or any self-reported difficulty with smell. All subjects reported typically falling asleep within 20 min and waking no more than once. Subjects were requested to sleep 2 h less than normal before the study day to facilitate their ability to fall asleep during the sleep phase of the study. Subjects were instructed not to consume alcohol or caffeine on the day of the study.

Data from three subjects were excluded due to inability to fall asleep ($n = 1$), inability to stay awake during fMRI scanning ($n = 1$) and reported inability to perceive odorants ($n = 1$). The reported results are based on data from the 15 remaining subjects (7 male, 24.5 ± 3.2 years, mean ± s.d.).

Awake control group. Subjects ($n = 15$) provided consent and were screened to take part in the study in the same manner as outlined for the sleep group. All subjects were age- and gender-matched to the 15 subjects in the experimental group (7 male, 25.6 ± 3.6 years, mean ± s.d.).

Stimuli. Grayscale photographs of men's faces, portraying neutral expressions, comprised the four CS cues (**Supplementary Fig. 1**). Assignment of faces to CS+, CS– and target or non-target conditions (see below) was counterbalanced across subjects. Mild electric shocks served as the US and were administered at conditioned stimulus offset to the dorsum of the left foot. Two conditioned stimulus cues were paired with the US (CS+) and two were never paired (CS–).

Two neutral odorants served as target and non-target contexts during CS presentations. To ensure that target and non-target odorants were equally familiar and neutral in valence, odorants were individually pre-selected on the basis of each subject's ratings of four odorants (limonene, α-pinene, acetophenone, and R-(–)-carvone, all approximately matched for intensity). Pleasantness and familiarity ratings did not significantly differ between target and non-target odorants (all $P > 0.08$). When asked to compare odorant intensities immediately following completion of each study phase, all but one subject reported that target and non-target intensities were equal.

Odorants were delivered via a 10-channel MRI-compatible, computer-controlled olfactometer (airflow, 3 l min^{-1}), minimizing tactile, thermal or auditory confounds[21]. Because odorant perception relies on nasal respiration, a small piece of surgical tape was placed vertically over subjects' closed mouths during the re-exposure phase. Assignment of pre-selected odorants to target and non-target conditions was randomized.

Electrical stimulation. Electrical stimulation intensity was calibrated per subject, such that stimulation was deemed "uncomfortable but tolerable" (mean intensity, 4.1 mA; s.d., 2.2; range, 1–11.5 mA; duration, 500 ms). Stimulation intensity did not differ between sleep and awake groups ($P > 0.84$). Stimulation was administered via a single square-wave pulse of current generated by a GRASS S-48 stimulator, delivered through bipolar Ag/Au electrodes[21].

Contextual conditioning procedure. In an fMRI contextual conditioning procedure, each CS+/CS– pair (target, non-target) was presented only in the context of its respective odorant (target, non-target). Thus, subjects learned to associate target/non-target conditioned stimulus pairs with the respective odorant context. During the pre-sleep conditioning task, tgCS+ and ntCS+ were paired with the US at 50% reinforcement, yielding paired (tgCS+p, ntCS+p) and unpaired (tgCS+u, ntCS+u) conditioned stimuli (**Supplementary Fig. 1a**). This allowed assessment of CS+-evoked responses without US interference.

Sessions began between 7:30 a.m. and 3:00 p.m. Following collection of odorant ratings, subjects entered the MRI scanner for the conditioning task. Stimuli were presented in a mixed design consisting of eight blocks (3 min per block). In each block, either the target or non-target odorant was continuously delivered and subjects were instructed to breathe through their noses. Target and non-target odorants were each delivered in four blocks, in pseudo-randomized order, such that no block of a single odorant was repeated more than once. Each block included eight CS+ trials (four CS+p, four CS+u) and eight CS– trials. All conditioned stimulus trials were presented in pseudo-random order for 1 s, followed by a jittered intertrial interval of 8–13 s during which a crosshair was displayed. Shock co-terminated with CS+p trials. All conditioned stimulus images were randomly presented 5 mm left or right of center, and subjects made a left or right response to each stimulus as quickly as possible by pressing one of two MRI-compatible buttons to ensure that they maintained attention. Responses were at least 95% accurate per scan for all subjects. Total duration of conditioning was ~29 min.

Following conditioning, subjects exited the MRI scanner and prepared for the sleep phase (~1.5 h after experiment start time). The target odorant was presented after the subject was judged to be in SWS (see below). To minimize stimulus habituation, the target odorant was administered in 30-s on/off intervals, following prior methods[2,4]. Following awakening, subjects were re-positioned in the scanner for the post-sleep retrieval task. This task was identical to pre-sleep conditioning, except that CS+/US pairing was at 12.5% reinforcement (to prevent fear extinction, as in previous studies[21]).

Following pre-sleep and post-sleep scans, subjects were asked to indicate which face images had 'sometimes' been paired with the US (CS+) and which had 'never' been paired (CS–) and to identify the odorant that had accompanied each. Following the pre-sleep conditioning task, subjects were 100% accurate in identifying the CS+ and CS–, and 94.2% accurate in identifying odorant contexts. Following the post-sleep retrieval task, subjects were 99.1% accurate in identifying the CS+ and CS–, and 94.8% accurate in identifying odorant contexts. There were no significant differences between subject groups (see below) for these results (all $P > 0.32$).

Awake control group. An awake group was included to test whether sleep had an essential role during target odorant re-exposure. Subjects in this group did not undergo fMRI scanning, but otherwise followed the same procedure as subjects in the original experiment. Start times for awake control subjects were yoked to those in the original experiment (within a 45-min margin of error), with no systematic differences between the two subject groups ($t_{14} = 0.926$, $P = 0.370$).

Awake control subjects completed the same pre-sleep conditioning task as in the original experiment, also showing increased SCR to CS+u versus CS– (main effect: $t_{14} = 3.61$, $P = 0.003$) with no effect of odorant context (stimulus × context interaction: $F_{1,14} = 0.63$, $P = 0.44$). During the re-exposure period, both timing and duration of target odorant delivery were yoked between subject groups. For those awake subjects whose matched sleep subject had experienced multiple re-exposure periods (due to multiple SWS cycles, $n = 4$), timing and duration were matched between subjects for all re-exposure periods. In place of sleep, awake subjects viewed a nature-themed documentary film to divert attention from odorant perception. Nevertheless, all 15 subjects in the awake group correctly identified the target odorant at the end of the study. In contrast, only 7 of 15 subjects in the experimental (sleep) group correctly identified the target odorant (as would be expected by chance).

SCR recording and statistical analysis. SCR was monitored continuously in the MRI environment using a PowerLab data-acquisition system (ADInstruments). Two MRI-compatible Ag-AgCl electrodes were placed on the left toes, following previously described methods[21,22]. SCR waveforms were sampled online at 1,000 Hz using high- and low-pass filters of 0.05 Hz and 1.5 Hz, respectively. Offline data analysis was conducted using Matlab (Mathworks). All epochs were extracted from the time of CS onset (with CS duration of 1 s) to 6 s post-CS offset, and were baseline-corrected in each trial by subtracting the mean SCR value during the 1s before CS onset. All paired CS+ (CS+p) responses were removed (due to signal interference from the US). Evoked responses were characterized by the peak-trough difference, where the peak was defined as the maximum amplitude 1–6 s after CS offset, and the trough as the corresponding lowest point (preceding the peak) in that epoch. In the case that no minimum preceded the peak (for example, a negative slope), the entire epoch was removed from analyses (which occurred in 25 of 3,240 cases). Within each run, raw values of peak-to-trough differences were transformed into percentage-change units, by comparing each value (X_i) to the minimum (X_{min}) and maximum (X_{max}) peak-to-trough difference within a run for each subject, where percentage change = $100 \times [(X_i - X_{min})/(X_{max} - X_{min})]$. To estimate the differential fear response for each subject, average CS– responses were subtracted from corresponding CS+u responses in each run. For group-wise analyses, a t test was used to compare pre-/post-sleep differences between target ($tgCS+u_{post\text{-}sleep} - tgCS+u_{pre\text{-}sleep}$)

doi:10.1038/nn.3527

versus non-target ($ntCS+u_{post\text{-}sleep} - ntCS+u_{pre\text{-}sleep}$) responses. A power analysis based on effect sizes reported using similar sleep-based reactivation methods[3] ($d = 1.50$, degrees of freedom = 12) indicated that a sample size of 14 was needed to detect effects of this magnitude (power = 0.80, $\alpha = 0.05$). For graphic depiction of variability estimates corresponding to the error terms used in within-subject statistical comparison (**Figs. 1** and **2**), error bars and box plots were adjusted for between-subjects differences by subtracting the mean across all conditions for each subject[3,23].

SCR was also collected during target odorant re-exposure (in both sleep and awake groups). Odorant-evoked signal was estimated by subtracting the peak SCR value for each 30-s odorant-off period from the peak value for the preceding 30-s odorant-on period. Raw values of odorant on/off differences were transformed into percentage-change units. Subsequently, SCR data were divided into first and second halves of the re-exposure period, individually per subject. For subjects with only one SWS cycle ($n = 11$), re-exposure consisted of a single block, split into halves according to its duration. In subjects with multiple SWS cycles ($n = 4$), re-exposure included multiple blocks that were later merged into one continuous block for split-half SCR analyses. For all subjects, mean SCR values for first and second halves of the re-exposure period were entered in a group (sleep, awake) × re-exposure period (first half, second half) ANOVA. Two subjects (one per group) were excluded from within-group analyses, due to excessive movement. For between-group comparisons, the participant yoked to each excluded subject was also removed to maintain matched re-exposure duration between groups. All between-group analyses were based on data from the remaining 13 subjects (per group).

Sleep recording and statistical analysis. EEG, electrooculographic and submental EMG signals were collected via a standard polysomnography (PSG) electrode montage. Signals were sampled online at 1,000 Hz, with high- and low-pass filters of 0.4 Hz and 30 Hz, using BrainVision Recorder (version 1.03) software. All data were compiled into 30-s epochs. Following online identification of two consecutive epochs characteristic of SWS, target odorant presentation was initiated, and was terminated at the first sign of awakening or change in sleep stage (according to standard PSG criteria)[24]. Detailed spectral analysis (**Supplementary Fig. 2**) was performed offline, using custom Matlab scripts in the EEGLAB[25] toolbox to identify delta (0–4 Hz), theta (4–8 Hz), alpha (8–12 Hz), beta (12–30 Hz) and gamma (30–40 Hz) bands. Periods of wakefulness, stage 1, stage 2, SWS and REM sleep were identified using PSG analysis (**Supplementary Table 3**) in accordance with standard criteria[24]. PSG was completed by an experienced rater (K.K.H.), blind to odorant onset/offset timing. Total duration of SWS (19 ± 3 min, mean ± s.e.m.) was consistent with prior studies using similar methods[3]. Duration of target odorant re-exposure (17 ± 3 min, mean ± s.e.m.) was negligibly less than SWS duration due to the necessity of first establishing accurate online assessments of SWS before administering odorant. The sleep phase concluded after subjects woke naturally or after at least 60 min had elapsed (73 ± 4 min, mean ± s.e.m.).

EEG data were analyzed using a combination of Matlab and EEGLAB[25]. Raw EEG data from odorant-on/odorant-off blocks were divided into 2-s, artifact-free epochs. Power spectral estimation of EEG signal was obtained using fast Fourier transforms with Hanning window tapering. The mean power at each frequency across blocks was compared for odorant-on versus odorant-off blocks, using two-tailed, paired *t* tests. Data from one subject were excluded due to lack of artifact-free epochs. Because there was no difference in effects between central electrodes C3 and C4, data were collapsed across these electrodes.

Data acquisition. MRI data were collected on a Siemens 3T-scanner, using a 32-channel head coil[21,22]. Functional data included whole-brain gradient-echo T2-weighted EPI (2-mm thick axial slices, 1-mm gap, repetition time = 1.510 s, echo time = 20 ms, flip angle = 75°, field-of-view = 220 × 206 mm, matrix = 128 × 120, in-plane resolution = 1.72 × 1.72 mm, voxel size = 2 mm^3). Image acquisition was tilted 30° from the horizontal axis to reduce susceptibility artifact in olfactory areas. A total of 1,144 volumes per run (for two runs) were collected in an interleaved ascending sequence (24 slices per volume). Whole-brain T1-weighted structural images were also collected (3D MPRAGE, voxel size, 1 mm^3).

Preprocessing. fMRI preprocessing and analysis were completed using SPM8. Image preprocessing included removal of the first six 'dummy' volumes (per run), spatial realignment (motion correction), and spatial normalization to a standard EPI template. For univariate analyses, images were spatially smoothed using a 6-mm full-width at half maximum Gaussian kernel. For multivariate pattern analyses, smoothing was not performed to preserve information at the level of individual voxels.

Univariate analyses. General linear models (GLMs) were created by modeling CS onset times using stick (delta) functions, and then convolving these functions with a standard canonical hemodynamic response function (HRF). This was performed for all 12 event-related regressors (tgCS+p, tgCS+u, tgCS–, ntCS+p, ntCS+u, ntCS–, for pre- and post-sleep). Temporal and dispersion derivatives of the canonical HRF were also included in these models. The six movement parameters derived from spatial realignment were included as nuisance regressors. Temporal auto-correlations were adjusted using an AR(1) process, and a 128-s high-pass filter removed low-frequency drift. Voxel-wise beta values for each condition were estimated from first-level models, for each subject individually.

Subject-wise comparisons (random-effects analyses) of parameter estimates were conducted using *post hoc* Student *t* tests. In a priori regions of interest (ROIs)[2,10,11], including hippocampus, amygdala, prefrontal cortex regions (ventromedial, orbitofrontal and dorsolateral PFC), piriform cortex, insula and ACC, significance thresholds of $P < 0.001$ (uncorrected) and cluster extent thresholds of $k > 2$ voxels were applied to group-level contrast images. The contrast of CS+u versus CS– was used to characterize neural correlates of pre-sleep fear conditioning. To model temporal effects during conditioning, we included corresponding trial-by-trial SCR values as a parametric regressor for each subject (**Supplementary Table 1**).

Next, we identified regions exhibiting post-sleep activity decreases in response to the target (tgCS+u) versus non-target (ntCS+u) stimulus, accounting for CS– baselines (to parallel the condition-specific decrease in SCR observed from pre- to post-sleep). Using a series of post hoc *t* tests, we examined the following contrast: $[(tgCS+u - tgCS-) - (ntCS+u - ntCS-)]_{pre\text{-}sleep} - [(tgCS+u - tgCS-) - (ntCS+u - ntCS-)]_{post\text{-}sleep}$ (**Supplementary Table 2**). A voxel-wise probability threshold of $P < 0.001$ (uncorrected) was applied. To guard against statistical non-independence due to multiple observations, we conducted a cross-validation analysis based on an iterative jackknife approach (leave-one-subject-out)[26], followed by small-volume correction. Small-volume correction was applied by centering a sphere (radius, 6 mm) on coordinates derived from the leave-one-subject-out analysis, and clusters passing a corrected threshold of $P < 0.05$ were reported (**Supplementary Table 2**).

A final univariate analysis identified regions in which the duration of target odorant re-exposure (during SWS) influenced the post-sleep tgCS+ (versus ntCS+) reduction. We first identified ROIs by using a flexible factorial model (SPM8), which identified brain regions exhibiting activity changes across all experimental conditions. Parameter estimates were modeled using a two-factor (subject, condition) ANOVA, correcting for non-sphericity. Omnibus *F* contrasts then revealed any subject-evoked mean fMRI activity changes across the experimental conditions. All ROIs passing a significance threshold of $P < 0.01$ (FWE-corrected) for this contrast were included in the subsequent correlational analyses. Two-tailed Pearson correlations were then performed, in which duration of odorant presentation in SWS (in minutes) was correlated with the post-sleep tgCS+ effect in the peak voxel for each region. A jackknife-based cross-validation approach was applied (**Fig. 2**)[26].

Multivariate pattern analyses. Multivariate analyses were performed to test whether re-exposure to odorant context during sleep led to altered patterns of fMRI ensemble activity[21,22]. First-level (single-subject) model estimation paralleled that for the univariate analyses, with the exception that normalized, but unsmoothed, functional images were entered into the GLMs, to preserve data at individual voxels. In these single-subject GLMs, odorant stimulus onsets for each condition and each fMRI run were modeled as delta functions, as described above. This resulted in eight total regressors per condition (four pre-sleep and four post-sleep). Beta values were then estimated from these GLMs and treated as spatially distributed patterns of brain activity in the following analyses.

Five ROIs were examined: amygdala, fusiform cortex, OFC, anterior piriform cortex (APC) and posterior piriform cortex (PPC)[10,21,22]. These ROIs were drawn in MRIcron software on an image constructed from the group average of the subjects' normalized T1-weighted scans. APC, PPC and amygdala were

identified based on anatomical landmarks following an anatomical atlas[27]. OFC was identified as a subregion of the larger OFC, centered on the intersection of the lateral, transverse and medial orbital sulci[10,21].

Beta values for all voxels in these ROIs were extracted from images corresponding to each condition-specific regressor in the single-subject GLMs and organized as linear vectors of voxel activity. This resulted in eight pattern vectors for each condition, ROI, and subject (four pre-sleep, four post-sleep). Uninformative voxels were removed by calculating a one-way ANOVA across all four conditions (tgCS+u, tgCS–, ntCS+u, ntCS–) in the pre-sleep data only, for each voxel. The voxels that passed this ANOVA ($P < 0.5$) were averaged across runs in each experimental phase, resulting in one pattern vector per ROI, subject, condition, and phase. Pairwise linear Pearson correlations were calculated between patterns evoked at pre- and post-sleep ($r_{pre,post}$) for all four conditions. These correlation values were examined for non-normality using Shapiro-Wilk tests; nonsignificant results (all $P > 0.257$) indicated that transformation was not necessary.

Correlation coefficients were then entered in a 2 × 2 ANOVA, to determine whether ensemble pattern correlations between pre- and post-sleep would vary as a function of the interaction between odorant context (target/non-target) and CS (CS+u/CS–). In a complementary analysis, correlation coefficients ($r_{pre,post}$) for both tgCS– and ntCS– were subtracted from the correlation coefficients for the respective CS+ (tgCS+u, ntCS+u) on a subject-by-subject basis, resulting in correlation difference values for target and non-target conditions. Tests of non-normality were nonsignificant (Shapiro-Wilk, all $P > 0.264$). Target versus non-target correlation values were thus analyzed via a paired two-tailed *t* test (**Fig. 2c**).

21. Li, W., Howard, J.D., Parrish, T.B. & Gottfried, J.A. *Science* **319**, 1842–1845 (2008).
22. Howard, J.D. *et al. Nat. Neurosci.* **12**, 932–938 (2009).
23. Cousineau, D. *Tutorials Quant. Meth. Psych.* **1**, 42–45 (2005).
24. Iber, C., Ancoli-Israel, S., Chesson, A.L. & Quan, S.F. (American Academy of Sleep Medicine, 2007).
25. Delorme, A. & Makeig, S. *J. Neurosci. Methods* **134**, 9–21 (2004).
26. Esterman, M., Tamber-Rosenau, B.J., Chiu, Y.C. & Yantis, S. *Neuroimage* **50**, 572–576 (2010).
27. Mai, J.K., Assheuer, J. & Paxinos, G. *Atlas of the Human Brain* (Academic Press, 1997).

doi:10.1038/nn.3527